Research, Society and Development, v. 11, n. 3, e25911326646, 2022
(CC BY 4.0) | ISSN 2525-3409 | DOI: http://dx.doi.org/10.33448/rsd-v11i3.26646

Chitosan/vancomycin antibacterial hydrogel for application in knee prostheses

Hidrogel antibacteriano de quitosana/vancomicina para aplicação em próteses de joelho

Hidrogel antibacteriano de quitosano/vancomicina para aplicación en prótesis de rodilla

Received: 02/07/2022 | Reviewed: 02/14/2022 | Accept: 02/14/2022 | Published: 03/07/2022

Fábio Gondim Nepomuceno
ORCID: https://orcid.org/0000-0001-7577-8894
Federal University of Campina Grande, Brazil
E-mail: gondimnet@gmail.com
Geceane Dias
ORCID: https://orcid.org/0000-0001-5997-3614
Federal University of Campina Grande, Brazil
E-mail: gd.dias@yahoo.com.br
Pascally Maria Aparecida Guerra de Araujo
ORCID: https://orcid.org/0000-0002-7268-7369
Federal University of Campina Grande, Brazil
E-mail: pascally.guerra@gmail.com
Líbia de Souza Conrado Oliveira
ORCID: https://orcid.org/0000-0001-6384-0793
Federal University of Campina Grande, Brazil
E-mail: libia.olivieira@ufcg.edu.br
Marcus Vinícius Lia Fook
ORCID: https://orcid.org/0000-0002-8566-920X
Federal University of Campina Grande, Brazil
E-mail: marcus.liafook@certbio.ufcg.edu.br
Ana Cristina Figueiredo de Melo Costa
ORCID: https://orcid.org/0000-0002-8585-0009
Federal University of Campina Grande, Brazil
E-mail: ana.figueiredo@professor.ufcg.edu.br

Abstract
Chitosan hydrogels stand out for being an adhesive matrix, which presents biocompatibility, antibacterial and osteogenic properties, biodegradability, non-toxicity, capable of retaining, releasing, and distributing therapeutic agents (drugs) at the application site. Therefore, new strategies in the field of orthopedics have focused, above all, on limiting the initial preoperative and postoperative microbial adhesion to implant surfaces, modifying these surfaces, protecting them from eventual adhesions or releasing the antimicrobial agent. The production of chitosan-based hydrogels has been achieved through physical and chemical cross-linking routes. In this context, this research aimed to develop an antibacterial hydrogel based on chitosan and vancomycin for application in total knee arthroplasty and to prevent bacterial infections. For that, three crosslinking procedures of chitosan with genipin were investigated to obtain the hydrogels and drug delivery. For this purpose, initially, the raw materials chitosan, genipin and vancomycin were characterized by infrared spectroscopy (FTIR), scanning electron microscopy (SEM), X-ray diffraction (XRD), pHmetry (pH) and microbiological tests. From the chemical crosslinking procedures evaluated, the drug release was investigated, and the hydrogels were characterized by FTIR, pH, viscosity, microbiology, and cytotoxicity. A new H5Q1GV hydrogel was obtained with good antibacterial activity, potentiated by the acidity of its pH 5.7, which showed good drug release in the first 4 hours after implantation, homogeneous, with ideal viscosity and adhesion for application through syringes in prosthesis surgery. knee and with excellent biocompatibility.
Keywords: Hydrogel; Chitosan; Vancomycin; Antibacterial; Knee prosthesis.

Resumo
Os hidrogéis de quitosana se destacam por ser uma matriz adesiva, que apresenta biocompatibilidade, propriedades antibacterianas, osteogênicas, biodegradabilidade, não toxicidade, capaz de reter, liberar e distribuir agentes terapêuticos (fármacos) no local de aplicação. Assim, novas estratégias no campo da ortopedia têm se concentrado, sobretudo, em limitar a adesão microbiana inicial pré e pós-operatória às superfícies dos implantes, modificando essas superfícies, protegendo-as de eventuais aderências ou liberando o agente antimicrobiano. A produção de hidrogéis à base de quitosana tem sido alcançada por meio de rotas físicas e químicas de reticulação. Neste contexto, este trabalho objetivou desenvolver um hidrogel antibacteriano à base de quitosana e vancomicina para aplicação em artroplastia total do joelho e evitar infecções bacterianas. Para tanto, foram investigados três procedimentos de reticulação da quitosana com a genipina para obtenção dos hidrogéis e carreamento de fármaco. Com essa finalidade, inicialmente, as matérias-primas quitosana, genipina e vancomicina foram caracterizadas por: espectroscopia no infravermelho (FTIR), microscopia

eletrônica de varredura (MEV), difração de raios-X (DRX), pHmetria (pH) e testes microbiológicos. A partir dos procedimentos de reticulação química avaliados foram investigados a liberação do fármaco e caracterizados os hidrogéis por FTIR, pH, viscosidade, microbiologia e citotoxicidade. Foi obtido um novo hidrogel H5Q1GV com boa atividade antibacteriana potencializado pela acidez do seu pH 5,7, que apresentou boa liberação do fármaco nas primeiras 4 horas após implantação, homogêneo, apresentando viscosidade e adesão ideais para aplicação através de seringas em cirurgia de prótese de joelho e com excelente biocompatibilidade.
Palavras-chave: Hidrogel; Quitosana; Vancomicina; Antibacteriano; Prótese de joelho.

Resumen
Los hidrogeles de quitosano se destacan por ser una matriz adhesiva, que posee biocompatibilidad, propiedades antibacterianas y osteogénicas, biodegradabilidad, no toxicidad, capaz de retener, liberar y distribuir agentes terapéuticos (fármacos) en el sitio de aplicación. Así, las nuevas estrategias en el campo de la ortopedia se han centrado, sobre todo, en limitar la adherencia microbiana inicial pre y postoperatoria a las superficies de los implantes, modificando estas superficies, protegiéndolas de eventuales adherencias o liberando el agente antimicrobiano. La producción de hidrogeles a base de quitosano se ha logrado a través de rutas de entrecruzamiento físico y químico. En este contexto, este trabajo tuvo como objetivo desarrollar un hidrogel antibacteriano a base de quitosano y vancomicina para su aplicación en artroplastia total de rodilla y para prevenir infecciones bacterianas. Para ello, se investigaron tres procedimientos de entrecruzamiento de quitosano con genipina para obtener los hidrogeles y la liberación de fármacos. Para ello, inicialmente, las materias primas quitosano, genipina y vancomicina se caracterizaron mediante: espectroscopía infrarroja (FTIR), microscopía electrónica de barrido (SEM), difracción de rayos X (XRD), pHmetría (pH) y pruebas microbiológicas. A partir de los procedimientos químicos de entrecruzamiento evaluados, se investigó la liberación del fármaco y se caracterizaron los hidrogeles por FTIR, pH, viscosidad, microbiología y citotoxicidad. Se obtuvo un nuevo hidrogel H5Q1GV con buena actividad antibacteriana, potenciada por la acidez de su pH 5.7, que mostró buena liberación del fármaco en las primeras 4 horas posteriores al implante, homogéneo, con viscosidad y adherencia ideal para aplicación mediante jeringas en cirugía de prótesis de rodilla y con excelente biocompatibilidad.
Palabras clave: Hidrogel; Quitosano; Vancomicina; Antibacteriano; Prótesis de rodilla.

1. Introduction

Osteoarthritis (OA) is the most common progressive musculoskeletal condition that can affect joints, and especially the hips and knees as the predominant weight-bearing joints (Hunter & Bierma-Zeinstra, 2019). Due to the higher prevalence of asymptomatic OA, it affects 250 million people worldwide. The prevalence of knee OA has increased significantly over the last few decades and continues to increase, in part due to the increased prevalence of obesity and other risk factors, but also independently of other causes (Carvalho Júnior et al., 2013).

It is estimated that the prevalence of knee OA among adults aged 60 years and over is approximately 10% in men and 13% in women and accounts for about 85% of the burden of osteoarthritis worldwide (Primorac et al., 2020). One of the treatments is replacement of the articular surface of the knee or arthroplasty surgery, a solution that has been tried since 1860, when soft tissue was interposed to reconstruct a joint with advanced arthrosis (Long et al., 2017; Miranda et al., 2012).

Recent Medicare data reported an increase in total knee arthroplasty volume from 9,650 in 1991 to 19,871 in 2010, while overall in the US it is projected that up to 270,000 total knee arthroplasty procedures will be performed in 45 years. Survival of primary total knee arthroplasties is well reported, with long-term survival greater than 95%. While failure rates and mechanisms for TKA revision are less well reported, over the long term, ranging from 71% to 96%. Given the increasing TKA revision rate, the economic burden associated with revision procedures is important to understand the reasons and risk factors for failure to focus efforts on improving revision durability (Geary et al., 2020).

There are no current epidemiological studies published in Brazil that quantify the number of surgeries performed to revision TKA. The survival rate and clinical outcomes of revision arthroplasties are lower than those of primary TKA, so that they should preferably be performed in specialized centers and with experienced surgeons. However, it is known that there is no such distinction for specialized centers in our environment, so that any service is authorized to perform these procedures. The main causes of failure are aseptic loosening, instability, and infection. (Lombardi Jr et al., 2014) reviewed 844 cases and found aseptic loosening in (31.2%) as the predominant failure mechanism in primary TKA, followed by instability (18.7%) and infection (16.2%), with an average time to failure of 5.9 years. This data is in line with those published by (Khan et al. 2016)

who reported cases of aseptic loosening (29.8%), infection (14.8%) and pain (9.5%) as the main indications for review.

Infection after total knee arthroplasty (TKA) represents a serious complication, with an incidence ranging from 0.5 to 3%. Such complication can have severe functional and psychological consequences for patients. Appropriate treatment remains controversial in the literature to this day, representing an enormous challenge for orthopedic surgeons. Patients with inflammatory symptoms for less than three weeks are classified as having a diagnosis of acute infection after TKA and are often treated with surgical splitting associated with intravenous antibiotic therapy. Success rates vary, and implant retention occurs between 44 and 84% of cases (Vivacqua et al., 2021).

Regarding the use of antibiotics used Filipović et al. (2020), shows the use of Vancomycin as a good indication in topical antibiotics to prevent infection in knee prostheses and emphasizes hydrogels as a good option.

As an infection prevention measure in TKA, the American Academy of Orthopedic Surgeons (AAOS) recommends systemic antimicrobial prophylaxis one hour before the surgical incision. However, the drug does not readily reach the implant-tissue interface. Therefore, local administration of antibiotics combined with systemic administration is recommended by some authors to provide higher concentrations of antibiotics *in situ*, with a lower risk of systemic toxicity (Cobra et al., 2021).

The most common microorganisms found in infection after TKA cultures are coagulase-negative *Staphylococcus* (30-43%) and *Staphylococcus aureus* (12-23%), followed by contamination by mixed flora (10%), *Streptococcus* (9-10%), *bacilli* gram negative (3-6%) and anaerobic (2-4%). No germ is isolated in about 11% of cases (Carvalho Júnior et al., 2013).

Researcher Florea et al. (2020), in turn, confirm the *Staphylococcus aureus* bacteria as the main cause of infection and the need for modified prostheses to prevent bacterial biofilm. In the studies by Perni and Prokopovich (2020) and (Osmani et al., 2021), researchers highlight the need for a new approach in the face of increasing antibiotic resistance in prosthesis infections and diabetes-associated infections that, even with medical advances, still present high morbidity.

Knowing that characteristics such as shape and type of prosthesis materials influence the possibility of bacterial contamination, the latest consensus on total knee prosthesis has motivated research to develop antibacterial surfaces that prevent adhesion, colonization, and subsequent bacterial proliferation (Cats-Baril et al., 2013).

Therefore, new strategies in the field of orthopedics have focused mainly on limiting the initial preoperative (Cai et al., 2017) and postoperative (Birt et al., 2017) microbial adhesion to the surfaces of the implants, for this patient are submitted to the use of antibiotics (Kapadia et al., 2016). However, many types of bacteria develop resistance to various antibiotics (Cox et al., 2016; Qi et al., 2017), especially when administered orally. Thus, a very attractive solution to minimize the use of antibiotics are bactericidal surfaces that can preventively kill bacteria in contact with the implant surface, protecting the site or releasing the antimicrobial agent and protecting the implant surface (Raphel et al., 2016).

Due to bacterial resistance to antibiotics, the literature reports that research has emphasized the development of biopolymer-based coatings for implants (Mishra et al., 2015), mainly due to their biocompatibility (He et al., 2017), being biologically based active (Iftime et al., 2017), and having antibacterial activity (Biao et al., 2017; Laskar et al., 2017; Mohamed et al., 2017; Wahid et al., 2017), among which we can mention: hydroxyapatite/chitosan/silicon composite coating on 316 L stainless steel implants with antibacterial and bioactive properties (Ordikhani et al., 2014); chitosan-silver nanocomposites used as an antimicrobial coating on titanium implants (Mishra et al., 2015), coatings to prevent infections associated with titanium implants such as antibiotic carriers to prevent biofilm formation (Rodríguez-Contreras et al., 2017).

In this sense, it is observed that, among the biopolymers used in orthopedic implants, chitosan stands out for its biocompatibility (Moura et al., 2017), antibacterial (Chang et al., 2017) and osteogenic properties (Lin et al., 2017), low cost (Vasilieva et al., 2017), biodegradability (He et al., 2017) and non-toxicity (Zubareva et al., 2017). It is highly promising for application in the biomedical area and in particular orthopedics (Kim et al., 2017; Yang et al., 2017), which can be in the form of gels (S. Wu et al., 2017), membranes (Carvalho et al., 2017), nanofibers (Sedghi et al., 2017), microparticles (Jeon et al.,

2016) and nanoparticles (Sáez et al., 2017).

Chitosan hydrogels in particular stand out for being an adhesive matrix capable of retaining, releasing and distributing therapeutic agents (drugs) at the application site. The methods for obtaining these hydrogels have been achieved through physical and chemical crosslinking routes (Jóźwiak et al., 2017), which causes changes in the physicochemical and mechanical characteristics of the structure (Xu et al., 2017), sterilization by plasma and gamma rays, which consists of establishing cross-links at specific points in the chains, increasing stability and maintaining the properties of the biopolymer (Mozalewska et al., 2017).

Recent studies report the use of chitosan for orthopedic applications, namely: Pawar et al. (2019), reported that the use of chitosan biomaterials carrying vancomycin has shown a promising and effective effect in the prophylaxis of infections in orthopedic surgeries due to the great potential for modifying the surface of surgical implants. In research by Ide and Ide and Farrag (2020) and Yousaf et al. (2020), the authors highlight the potential use of chitosan as a drug carrier to fight infection. Kumar et al. (2021), emphasized the success of chitosan in combating *Staphylococcus aureus*. However, although recent studies have made great progress in exploring the antibacterial properties of modified surfaces, the practical applicability in orthopedic surgery is still very limited.

Therefore, this work aimed to develop a chitosan hydrogel chemically cross-linked with genipin and carrying the drug vancomycin and further characterized by structural, rheological, microbiological, biocompatibility and drug release analysis were performed to assess the real antibacterial benefit and of antibiotic release to be used in knee arthroplasty surgeries and to avoid bacterial infections.

2. Methodology

To produce the hydrogel, the methodology described by Solé et al. (2017), in "Patent Translate" CN105920675 and CN105968388 and Mi et al. (2000), was considered as reference, which makes use of a 1.5% (m/v) chitosan solution, where 1.5g of chitosan were dissolved in 100mL of 1% (v/v) lactic acid solution, and later addition of the drug vancomycin using the methodology described by (Talebian & Mansourian, 2017).

The materials used were: low molecular weight chitosan (Q1) with an approximate degree of deacetylation of 90%, provided by CERTBIO (De Queiroz Antonino et al., 2017); low molecular weight chitosan (Q2) with an approximate degree of deacetylation of 92.5% purchased from Sigma-Aldrich; lactic acid with purity greater than 98% (Sigma-Aldrich); genipin (G) with purity greater than 98% (Sigma-Aldrich); vancomycin hydrochloride (V), lyophilized powder, TEUTO 500mg/vial ampoule; water for injection (Fresenius Kabi Brasil), pH between 5 and 7; and phosphate buffer saline (PBS) pH 7.4;0.1M.

The hydrogel was obtained in a room standardized by the Brazilian pharmacopoeia (ANVISA, 2010), which is where the concentration of airborne particles is controlled and in which other relevant parameters, such as temperature and humidity, can be constantly monitored and controlled. In the entire experimental process to obtain the hydrogel, pipettes, beakers, and magnetic stirrers sterilized in a Baumer brand autoclave for 15min at 127ºC were used. The water used was standardized according to the Brazilian pharmacopoeia (ANVISA, 2010), and met the physicochemical tests recommended for purified water, in addition to the total bacterial count < 10 CFU/100mL, sterility, particulate and bacterial endotoxin tests, whose maximum value is 0.25IU of endotoxin/mL.

To produce the hydrogel, first a base solution was prepared by dissolving the polymer chitosan in lactic acid (1% v/v), for a final concentration of the polymer solution (1.5% m/v), under magnetic stirring, Fisatom model at 840rpm/1h, at a temperature of 25ºC, closed dome to avoid contaminants and, afterwards, kept at rest for 30min. This was the base solution used to form the hydrogel.

The crosslinking of the base solution, by the crosslinking agent genipin and the addition of the drug vancomycin, was

performed in three distinct sequences:

R1 - The drug was added together with the crosslinking agent to the chitosan solution. 20mL of the chitosan solution was taken and 0.2g of the drug vancomycin and 0.012g of the cross-linking agent genipin dissolved in 2mL of distilled water were added under stirring. The solution was kept under magnetic stirring at 840rpm for 12h. After all this process, 20g of the hydrogel was obtained with the following composition: 1.5% (m/m) of chitosan; 1% (w/w) drug and 0.06% (w/w) genipin.

R2 - The drug was first added to the chitosan solution and then crosslinked after. From the chitosan solution, 20mL was withdrawn and, under stirring, 0.2g of the drug vancomycin was added, dissolved in 1mL of distilled water, keeping under stirring for 4h. After this time, still under agitation, 0.012g of the crosslinking agent genipin was added, dissolved in 1mL of distilled water, and left under agitation for 12h at 840rpm. At the end of the process, 20g of hydrogel of composition: 1.5% (m/m) of chitosan was obtained; 1% (w/w) drug and 0.06% (w/w) genipin.

R3 -The crosslinking agent was added first to the chitosan solution and then the addition of the drug vancomycin was carried out. From the chitosan solution, 20mL was removed and, under stirring, 0.012g of the crosslinking agent genipin dissolved in 1mL of distilled water was added, keeping under stirring for 4hrs. Then 0.2g of the drug vancomycin dissolved in 1mL of distilled water was added. Stirring continued for another 8hrs at 840rpm. After all this process, 20g of hydrogel with composition were obtained: 1.5% (m/m) of chitosan; 1% (w/w) drug and 0.06% (w/w) genipin. The quantities of raw materials are summarized in Table 1.

The hydrogel was stored under refrigeration at 6ºC and showed good workability characteristics. The raw material used to obtain the hydrogel was characterized by X-ray diffraction using a BRUKER model D2 Phaser X-ray diffractometer, (Cu Kα radiation), voltage of 40kV, 30mA current, with scanning $5° \leq 2\theta \leq 50°$ with an increment of 0.016. The FTIR spectra of the raw material and of the hydrogels were obtained using a Vertex 70 – Bruker model spectrometer, between 4000 and 650cm^{-1}, is excellent for evaluating polymers, it helps in the identification of molecular compounds and their chemical composition, provides evidence of the presence of functional groups present in the structure, making it possible to understand the interactions of raw materials in the final product. The morphology of the raw materials was analysed by Hitachi with model TM-1000 scanning electron microscopy.

Table 1 - Composition of raw materials, procedure and time used in the production of hydrogels.

Hydrogel	Q1 (g)	Q2 (g)	G (g)	V (g)	Crosslinking	Time (h)
HQ_1G	1.5	-	0.5	Não	R1	12
HQ_2G	-	1.5	0.5	Não	R1	12
H_1Q_1GV	1.5	-	0.1	2.0	R3	24
H_2Q_1GV	1.5	-	0.1	1.0	R3	6
H_3Q_1GV	1.5	-	0.1	1.0	R3	12
H_4Q_1GV	1.5	-	0.8	0.5	R1 R2 R3	8
H_5Q_1GV	**1.5**	**-**	**0.06**	**1.0**	**R3**	**8**
H_6Q_1GV	2.0	-	0.01	1.0	R3	12
H_7Q_1GV	2.0	-	0.008	1.0	R3	24
H_8Q_1GV	1.5	-	0.06	1.0	R3	12
H_1Q_2GV	-	1.5	0.06	1.0	R3	8
H_2Q_2GV	-	1.5	0.04	1.0	R3	12
H_3Q_2GV	-	1.5	0.04	1.0	R3	8
H_4Q_2GV	-	1.5	0.03		R3	8
H_5Q_2GV		1.5	0.06	1.0	R3	8

*R – crosslinking procedure. Source: Research Data.

The antimicrobial activity of chitosan is closely related to its physicochemical properties as described in the literature review, in particular the pH. In this sense, the pH of the hydrogel was measured with a pH meter from the AKSO AK90 brand (for a pH around 6.0). All raw materials were subjected to pH tests to achieve a final product with a maximum pH of 6.2 being of low local toxicity and at the same time allowing the bactericidal effect of chitosan. Preliminary microbiological tests for the

absence of biological contaminants were carried out at the Prosangue Diagnostic Laboratory and Medical Center – Campina Grande Unit. The following samples were analysed: chitosan, vancomycin, genipin, lactic acid and the chitosan and chitosan hydrogel carrying vancomycin illustred in (Figure 1).

Figure 1 - Materials for testing the absence of contamination.

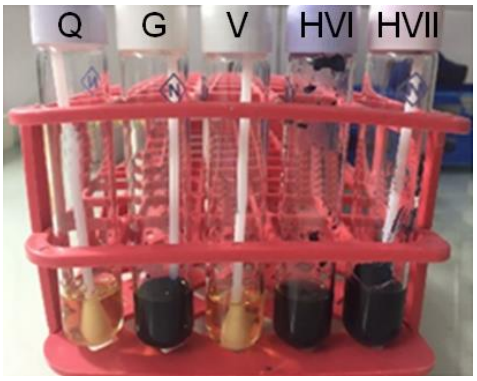

Source: Research Data.

The samples were immersed in tubes containing 5mL of a liquid medium enriched with BHI (Brain-Heart Infusion), which allows the proliferation of microbial cells, aiming to increase the number of bacteria present in the samples. The BHI tubes were incubated in a bacteriological incubator at a temperature of 35º ± 2ºC for 24h. After the incubation period with the aid of sterile flexible rods, the samples immersed in BHI were seeded on plates containing Sheep Blood Agar medium, as this medium has a rich and supplemented base providing the adequate growth of gram-positive bacteria, gram-negatives and fungi. The seeded plates were incubated in a bacteriological incubator at a temperature of 35º ± 2ºC for 48h and in the reading, they did not show growth of bacteria and fungi/yeasts in the analysed materials.

Certified microbiology on the final product was performed at CERTBIO with a count of total number of mesophilic microorganisms in the chitosan hydrogel without the drug vancomycin to assess contamination with fungi/yeasts or bacteria. The sample was handled in a sterile environment using the Quimis biological safety cabinet. For the assay, casin-soy agar (casein-soy broth) and sabouraud-dextrose agar (Kasvi – Italy) were used. The verification of microorganisms was performed by counting the total number of mesophilic microorganisms, a methodology recommended by the Brazilian Pharmacopoeia (ANVISA ,2010). The determination was carried out by the plate method and there was no growth of bacteria and fungi/yeasts in the material analysed (chitosan hydrogel crosslinked with genipin).

The hydrogel was submitted to in vitro tests to evaluate the antibacterial activity of pure chitosan and associated with vancomycin, using the classic technique with disk diffusion or the Kirby-Bauer test due to its practicality, cost compatible with the research budget and proven efficiency being the most used method in the world to assess the antimicrobial effect. The test was carried out at CERTBIO, being handled in a sterile environment using the biological safety cabinet of the Quimis brand, following the Brazilian Pharmacopoeia (5th edition). Mueller HintonBroth culture medium (Mueller Hinton-Kasvi–Italy Broth) was used for the assay, added with solidifying medium (Bacto Agar – BD) and tested according to the requested method (disk diffusion). The samples were tested against the strain of interest in knee surgery: Staphylococcus aureaus ATCC 25923. The bacterial growth on the agar plates showed that the bacteria were actively developing their colonies.

The hydrogel sample with vancomycin and chitosan (HG2); the positive control with vancomycin (C+V) and the negative control with saline solution (C) were distributed on the surface of the Agar, which was then incubated in a bacteriological incubator at a temperature of 35º ± 2ºC for 24 hours and 48 hours in triplicate.

After the incubation time, the reading and interpretation of the results was performed, observing the presence or not of growth inhibition halos, a clear circular zone, without growth in the vicinity of the hydrogel, indicating an antimicrobial effect and through reference tables, the size of the zone in millimetres can be related to the MIC and assessed whether the organism is susceptible or resistant to the antimicrobial agent.

Tests for drug release were performed discontinuously, with agitation and controlled temperature. One gram of hydrogel, already containing the drug, was weighed, placed in a 250ml Erlenmeyer flask, added 20ml of phosphate buffer pH7, taken to a shaker incubator under stirring at 200 rpm and at a controlled temperature of 36°C. A sufficient quantity of samples was prepared so that the kinetic monitoring of the drug release was carried out until the equilibrium condition was reached. Every 5 minutes, an Erlenmeyer flask was removed from the shaker incubator, the hydrogel was separated from the solution using a commercial sieve, and the translucent liquid was subjected to spectrophotometric analysis at the wavelength in the UV region of 284nm to quantify the concentration of vancomycin in the solution. The absorbance value was correlated with the concentration by means of a calibration curve previously obtained with the solution of a known concentration of vancomycin, in the linear region, as recommended by the Lambert-Beer Law.

The percentage of drug released over time was obtained by Equation (1) shown below. For the balance of mass, it was assumed that all the vancomycin introduced during the preparation of the hydrogel was retained by the hydrogel until the moment of release.

$$\%Released = \frac{M_t}{M_i} x100 \quad \text{Eq. (1)}$$

Where:

% Released - percentage of drug released over time.

M_t – Drug mass released in the buffer solution over time.

M_i - Drug mass initially placed in the hydrogel.

It should be noted that the maximum percentage released must be equal to the initial amount of vancomycin introduced into the hydrogel. Release tests were performed in duplicate, starting from the same hydrogel (drug-carried) with an interval of 7 days. During this period, the hydrogel was placed in a glass container, sealed, and kept in a refrigerator.

The readings of absorbances of the hydrogel (drug carriers) were carried out in a Bel Photonics 2000 UV spectrophotometer, in the region of the maximum wavelength of 284nm. This length was determined after scanning the drug solution in the spectrophotometer in the range from 210 to 300nm, as detailed in Appendix A. Based on this reading, the calibration curve was obtained and the correlation in the linear range of the Lambert-Beer law, Absorbance x Concentration was used to quantify the drug concentration in the release experiments. The maximum amount of vancomycin hydrochloride (vancomycin) that must be released into each hydrogel (carrier system) can be equal to the amount of mass initially placed in each composition. Therefore, it is possible to determine the drug mass, which is released, through a mass balance applied between the buffer solution and the hydrogel, of known mass, used for release.

The hydrogel obtained was subjected to a viscosity test in a Haake Mars III Rheometer (Karlshuhe, Germany) manufactured by Thermo Scientific with Type of Geometry in Parallel Plates with a trap for solvents with a diameter of 60mm, carried out at a temperature of 25ºC and 35ºC. The oscillatory test was carried out, with a deformation of 0.1% in the frequency range from 0.1 to 100Hz, to determine the complex viscosity as a function of frequency. Optimal viscosity was determined by the force required to allow the hydrogel to allow application through injection syringes illustred in (Figure 2).

Figure 2 - Syringe to test hydrogel fluidity.

Source: Research Data.

Seeking to assess the feasibility of using the hydrogel (chitosan/genipin) as a carrier system for the drug vancomycin, the in vitro analysis will be investigated through cytotoxicity assays.

The purpose of performing the cytotoxicity test is to assess the potential of a material to produce adverse effects on biological systems at the cellular level that could damage the cells or reduce the rate of cell growth in the culture. A fibroblast culture (L929) Norm (ISO 10993-5: (2009)(Standardization, 2009), was used, using a laminar flow chamber; incubator; spectrophotometer; inverted optical microscope and automated cell counter.

Cytotoxicity testing can be performed in three ways: the elution test, the direct contact test and the agar diffusion test. In the present work, the indirect agar diffusion test was used, and its effect was evaluated by the sample through the agar layer, which protects the rat connective tissue cells (L-929 cell line fibroblasts) from mechanical damage during placement of the sample and allows diffusion of chemicals that migrate from the polymer samples.

The agar diffusion method (Cytotoxicity assay), in vitro cytotoxicity assay, was the most suitable for evaluating the safety of plastic materials, elastomers, and other polymers, used in the manufacture of devices and accessories for medical and hospital use in direct contact or indirect with human tissue.

The samples were sterilized by ultraviolet radiation in a BIOGREEN laminar flow cabinet for 1h, in a 30-min cycle for each side of the sample. In this way, the samples were standardized with an area of approximately 100mm² (10mm x 10mm). Then, positive controls (Latex for tourniquet) and negative controls (Whatman filter paper n.01 or HDPE - High Density Polyethylene) were prepared.

A suspension of L-929 cells with concentrations ranging from 1.1 to 1.3 x 105 viable cells per ml in RPMI 1640 medium containing 10% fetal bovine serum (FBS) was used for the assay. Four milliliters of the cell suspension obtained were placed in each hole of the plastic culture microplate (3.5cm in diameter). Then, duplicate cultures were prepared for the sample, negative control, positive control and blank. Cultures were incubated at 37°C ± 1°C with 5% ± 1% CO_2.

Approximately forty-eight hours after the establishment of cultures, those with a uniform cell monolayer and close to confluence (greater than 80% confluence) were used for the assay. Therefore, the culture medium of the microplates was aspirated, the monolayer of each plate hole was washed with 2mL of PBS solution, which was then also aspirated, 1mL of covering medium was added to each well, this medium is composed on 1.8% agar, added with 0.01% neutral red dye and concentrated 2X MEM, in equal amounts. The plates remained in the laminar flow hood for 10 min, waiting for the agar to solidify at room temperature.

Therefore, the standardized samples obtained from the respective material, the negative control and the positive control, in duplicate cultures, were placed in contact with the solidified surface of the agar, in the center of each plate.

Thus, the plates were incubated in an inverted position, wrapped in aluminum foil to avoid cell damage by photoactivation of neutral red (ISO 10993-5)(Standardization, 2009), for at least 24 hours in an oven at 37°C ± 1°C, humidified and with 5% ± 1% of CO_2 for evaluation of cytotoxicity.

The evaluation of cytotoxicity took place twenty-four hours after the application of the Sample, microscopically observing the morphology and coloring of the cells under and around the samples to be tested and the Controls. The extent of the discolored area (dead cells) from the ends of the sample in the 4 different quadrants was measured macroscopically with the aid of a caliper. The mean value of the values of the 4 different quadrants was calculated. The mean values obtained for each sample and controls with the specified limits for the different degrees of cytotoxicity indicated in Table 2.

The degree of cytotoxicity is rated on a scale from 0 to 4 according to Table 2, the neutral red vital dye added to the overlay medium is rapidly taken up by living cells, stored in lysosomes (Grasso et al., 1973), staining those cells in red, during the necrosis process the stained cells release the dye producing regions with discolored dead cells.

Table 2 – Degrees of cytotoxicity.

DEGREE	CYTOTOXICITY	DESCRIPTION OF THE CYTOTOXICITY ZONE
0	Absence	Absence of discoloration around or under the sample.
1	Light	Bleaching zone limited to the area under the sample.
2	Soft	Size of the bleaching zone from the sample less than 0.45cm.
3	Moderate	Size of the bleaching zone from the sample between 0.45cm to 1.0cm.
4	Severe	Size of the bleaching zone from the sample greater than 1.0cm, but not involving the entire plate.

Source: Research Data.

3. Results

Figure 3 shows the X-ray diffractograms of chitosan (Q1) and (Q2), genipin (Gp) and vancomycin (V). From the diffraction spectra (Figure 3a and 3b), two crystalline peaks can be observed at 2θ = 10.7° less intense and with a broader aspect, and at 2θ = 20.6°, with a peak characterized with a greater intensity consistent with chitosan standards in the literature. According to these characteristics we can say that chitosan is considered a material semi-crystalline.

Figure 3 - X-ray diffractogram: (a) and (b) chitosan (Q1) and (Q2), (c) vancomycin (V) and (d) genipin (Gp).

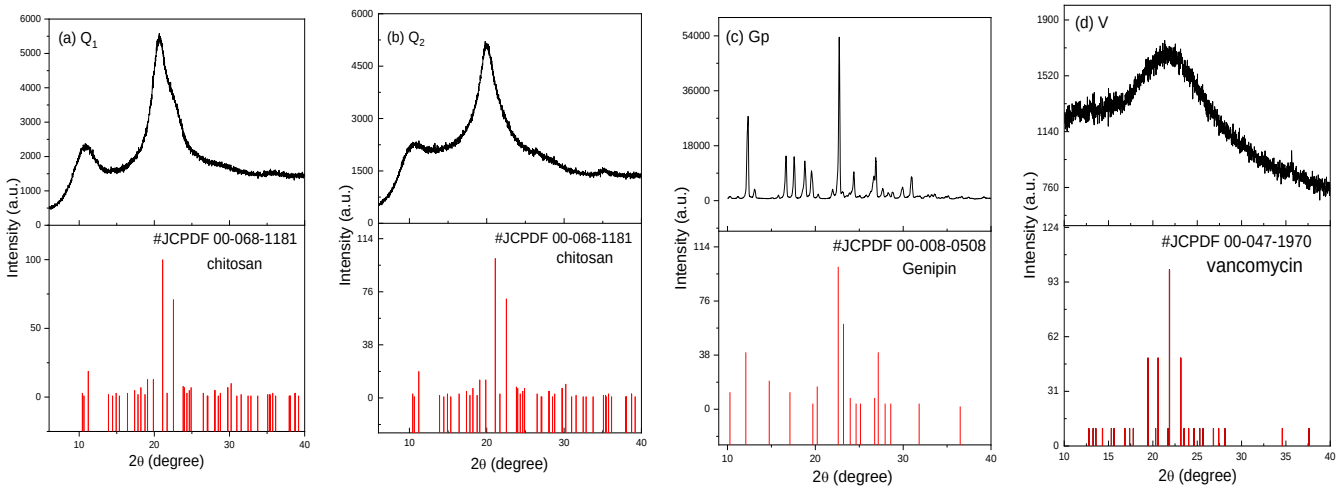

Source: Research Data.

According to the researchers: Saita et al. (2012), Huang et al. (2017), Bakshi et al. (2018) and (Fan et al., 2018), the crystallinity observed in chitosan is explained by the fact that its molecular structure presents certain regularity and also the presence of -NH_2 and OH groups that provide strong intermolecular and intramolecular hydrogen bonds, which ends up causing more stability and ordering in the structure polymer chain, and as a result the presence of crystalline regions in the molecular

structure of chitosan. These same peaks and characteristics were also observed in the diffractograms obtained by Fan et al. (2018), when performing the synthesis of chitosan derivatives from the grafting of polyaminoethyl and diethoxyphosphoryl groups as a strategy to improve the protonation potential and thus increase the antifungal activity of chitosan and by Li et al. (2013), by synthesizing a complex of cross-linked chitosan with glutaraldehyde in order to assess the antibacterial activity against the Burkholderia Cepacia Complex (BCC). Demetgül and Beyazit (2018), also observed when synthesizing a chitosan modified with a chromone-chitosan Schiff base (CSCH) and its derivative cross-linked with terephthalaldehyde (TP) to evaluate its antioxidant effect, they also observed these peaks.

Figure 3d illustrates the X-ray diffractogram of the crosslinking agent genipin (Gp). One can observe sharper and more intense peaks representing greater crystallinity. Little is said in the literature about the structural characterization of genipin by XRD, but these same characteristics were observed by Zeng et al. (2015), by synthesizing silk fibroin microspheres with chitosan using different concentrations of the crosslinking agent genipin, and performing a comparative study with pure chitosan microspheres regarding encapsulation efficiency and controlled release rate, and with this also seeking to analyse the physical and chemical properties of microspheres.

The studies by Luo et al. (2015), showed when preparing chitosan microspheres by the emulsion crosslinking method using genipin (Gp) for in vitro studies of controlled release of salidroside and Zhang et al. (2011), when carrying out a comparative investigation regarding the intestinal absorption of the inclusion complex genipin/hydroxypropyl-β-cyclodextrin (HP-β-CD) with that of genipin, they also observed the same characteristic peaks in the X-ray diffraction of genipin.

In Figure 3d is the X-ray diffractogram of vancomycin (V). One can observe a band at 2θ = 15° to 30° and absence of peaks indicating the amorphous characteristic of the material. This same observation was reported by (Jarquín-Yáñez et al., 2017), when performing an optimization by a 23-factorial experiment in chitosan microparticles to serve as a vancomycin carrier for possible application in the treatment of periodontal diseases; and by Saidykhan et al. (2016), by developing a system with aragonite nanoparticles, derived from cockle bark, loaded with vancomycin for the treatment of osteomyelitis. The amorphous character of vancomycin was also observed in the X-ray diffractogram exposed in the work of Rahman and Khan (2013), when evaluating the variability of the product of a soluble dispersion formulation of a peptide antibiotic.

Figure 4 illustrates the infrared spectra of the raw materials chitosan (Q1) and (Q2), genipin (Gp) and vancomycin (V). It can be observed in the spectra referring to chitosan (Q1) and (Q2) (Figure 4a and 4b) a wide band around 3000 – 3600cm-^{1} with maximum intensity in 3255cm-^{1} attributed to the axial elongation vibrations of the OH groups that appear superimposed on the band elongation of the NH groups, as well as the intermolecular hydrogen bonds of the polysaccharide chains. The band at 1649cm-1 is associated with the elongation vibration of the C=O carbonyl group of the amide groups (amide I), present in the acetylated units of chitosan, and the absorption band around 1581cm-^{1} is related to the overlap of two vibrations: the vibration of the amide group (called amide II) and the deformation vibration of the NH bond of the primary amines present in the deacetylated units. The band at 1374cm-^{1} is assigned to the CH_3 group. The existence of the C=O and N-H bands together indicate the presence of amide groups. In the range 1122 - 512 possibly these are pyrosidic rings.

The band around 1150cm^{-1} is attributed to the asymmetrical elongation of the C-O-C group which is characteristic of the polysaccharide structure (Dimida et al., 2017; Lai et al., 2010). Bands at 1066 and 1028cm^{-1} refer to vibration involving C-O elongation. In the range of 1384-1308cm^{-1} there is an absorption that can be attributed to the symmetric deformation of C-H.

The vibrations between 1233 and 1000cm^{-1} are attributed to the stretching (C-O-) of alcohols. The 900cm^{-1} absorption is related to the presence of C-H. At approximately 1422cm^{-1}, a signal regarding the absorption of symmetrical elongation of carboxylic acid salts can be detected. The bands around 2960 and 2876cm^{-1} are caused by elongation vibrations of the C-H group (Demetgül & Beyazit, 2018).

These characteristic FTIR bands for chitosan (Q1) and (Q2) corroborate the results observed by: Delgadillo-Armendariz

et al. (2014), when investigating the absorption characteristics of the drug glibenclamide in hydrogelchitosan/genipin. Researchers Sami et al. (2018), when formulating a hydrogel based on the biopolymers chitosan and guar gum for an evaluative study of the controlled release of the analgesic Paracetamol. Bakshi et al. (2018), when carrying out a comparative study of the antimicrobial activity and biocompatibility of N-selective chitosan derivatives.

Figure 4 - FTIR spectra: (a) and (b) chitosan (Q1) and (Q2), (c) genipin (Gp) and (d) vancomycin (V).

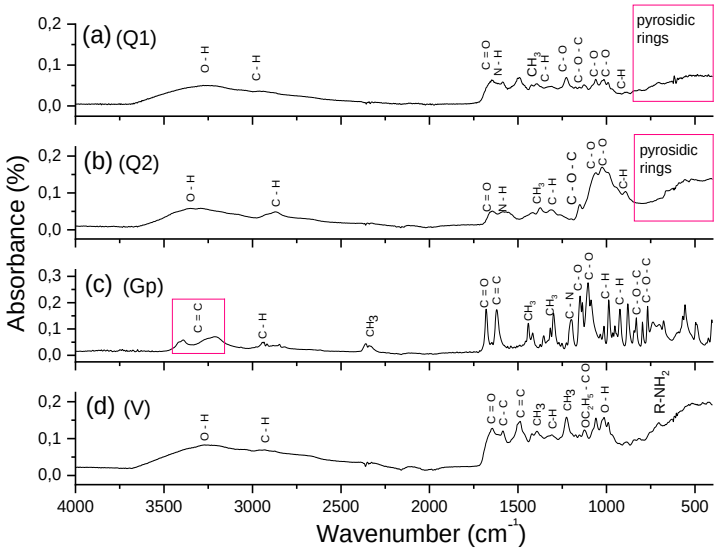

Source: Research Data.

Related to the FTIR spectrum shown in Figure 4c referring to genipin one can observe the absorption band at 1680cm-1 which is attributed to the elongation vibration of the C=O bond in the carboxylic groups esterified with the methyl group, while the absorption at 1619cm-1 is related to the elongation vibration of the cycloolefin alkene ν(C=C) of the genipin molecule core. The absorptions at 2343 and 1200cm-1 are attributed to CH_3 elongation strain and C-N elongation vibration respectively. The absorption band at 1445cm-1 corresponds to the flexion of the CH_3 bond and the absorptions at 1150 and 1104cm-1 are associated with the elongation vibration of the ν(C-O) group in the cyclic ether of the structure. The absorption at 2942cm-1 is attributed to the elongation of the C-H group. In the range between 3397-3211 it is assigned to the C=C group. The absorption band between 997-925cm-1 was assigned to the C-H ring's out-of-plane curvature mode, and the absorption at 1308cm-1 is related to CH_3 flexion.

The absorption at 771cm-1 is related to the mode of curvature of the C-O-C out of plane. The attribution of characteristic bands of the FTIR spectrum to Gp were also observed by Dimida et al. (2017), when they produced scaffolds for bone regeneration and repair of crosslinked chitosan with different concentrations of genipin for evaluation of physical, chemical and biological properties and by Delgadillo-Armendariz et al. (2014), when investigating the absorption characteristics of the drug glibenclamide in hydrogelchitosan/genipin.

By means of the FTIR spectrum of vancomycin Figure 4d it is possible to observe the absorptions occurring in 3270, 1649 and 1490cm-1 are related to the presence of O-H, C=O, C=C, respectively. The absorption bands at 2936 and 1310cm-1 are attributed to the axial deformation of the C-H group and possibly associated with the C-H group respectively. In the absorption range between 1420-1393 it is related to the asymmetric deformation of CH_3. The absorption bands at 1228 and 1125 cm-1 are assigned to the CH_3 and OC_2H_5-CO groups, respectively, while the absorption at 1589cm-1 is related to the C-C aromatic vibration. The absorptions occurring at 1014 and 718cm-1 are related to the O-H and R-NH_2 groups, respectively.

These same vancomycin bands were observed by Yao et al. (2013), when developing scaffolds by the replication

technique using 45S5 Bioglass® (BG) coated with polycaprolactone and chitosan loaded with vancomycin for application in bone tissue engineering and by López-Iglesias et al. (2019), when conducting evaluative studies on the ability of chitosan aerogels loaded with vancomycin to act as a potential formulation to treat and prevent infections in chronic wounds.

Figure 5 presents the morphological characterization of the raw materials chitosan (Q1) and (Q2), genipin (Gp) e vancomycin hydrochloride, (V).

Figure 5 – SEM: (a) and (b) chitosan (Q1) and (Q2), (c) genipin (Gp), and (d) vancomycin hydrochloride (V).

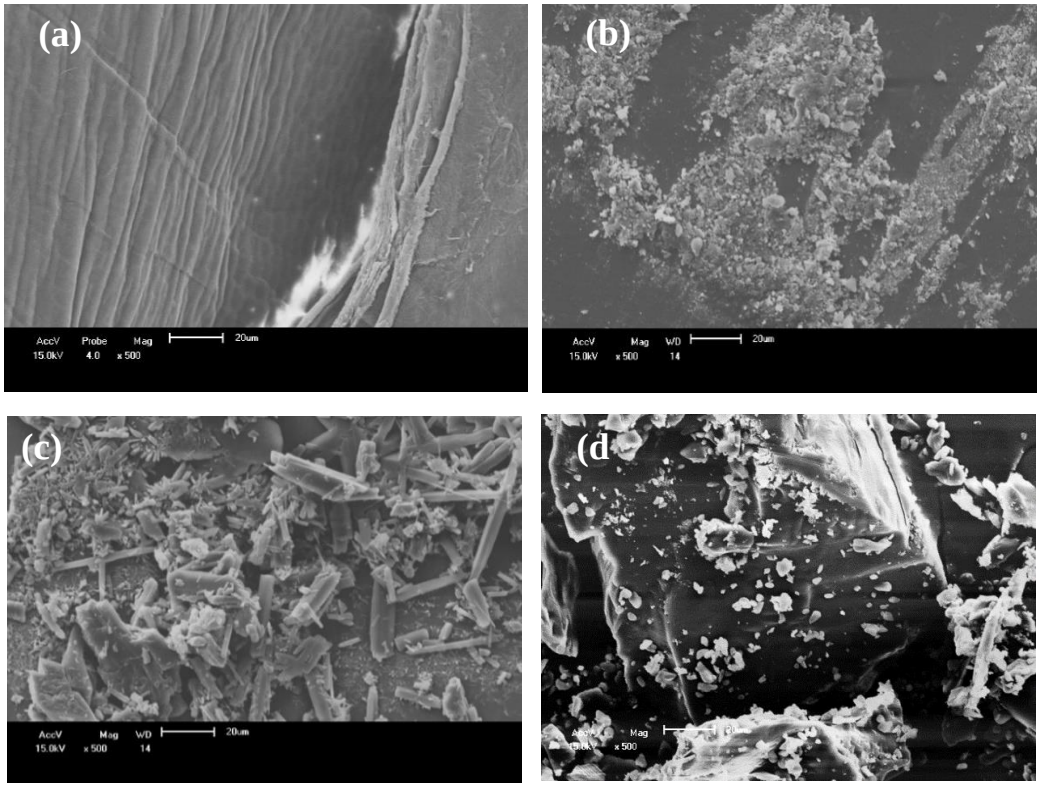

Source: Research Data.

Through the micrograph of chitosan (Q1) (Figure 5 [a]) it is possible to observe an irregular surface with roughness and characteristics of a non-porous and dense surface. These morphological characteristics of chitosan were also observed by: Demetgül and Beyazit (2018), when they synthesized a new Schiff base of chitosan-chromone (CSCH) and its cross-linked derivative (CSCH-TP) by the condensation reaction of 6-formyl-7-hydroxy-5-methoxy-2-methylbenzopyran-4-one (CH) with chitosan (CS) and terephthalaldehyde (TP) as crosslinking agent. Trimukhe and Varma (2008) when preparing metal complexes of Hg, Cu, Cd, Pb, Zn and Mn salts with chitosan and cross-linked chitosan to study their morphologies. Researchers Li et al. (2013), by synthesizing and characterizing a complex of chitosan crosslinked with glutaraldehyde to evaluate the antibacterial activity.

The micrograph of genipin (Gp) (Figure 5c) reports a morphology with an irregular surface and the presence of rod-shaped clusters evidencing a crystalline material. This result corroborates the X-ray diffractogram of genipin (Figure 5 c). These same characteristics were also observed in the study by Saikia et al. (2016), when synthesizing starch-coated magnetic iron oxide nanoparticles loaded with curcumin and cross-linked with glutaraldehyde, genipin and citric acid.

The Figure 5d shows the morphological characterization of the drug vancomycin hydrochloride. It is possible to observe micrometric particles of irregular, non-uniform appearance (indicated by green arrows) and around these particles there is a region of darker void. These same observations were made in studies by Park et al. (2013), when designing aerosol dry powder inhalers, co-spray-dry (microparticulates/nanoparticulates loaded with vancomycin and clarithromycin.

The test results for biological contaminants of the chitosan (Q1), genipin (G), vancomycin (V), lactic acid (AcL) and contaminated water samples for positive control are shown in Figure 6. It can be observed that the raw materials Q1, G, V and AcL did not show colony growth on blood agar culture medium (uniform red coloration) (Figure 6b, c, d, e), however, the contaminated positive control showed exuberant growth of biological contaminants (Figure 6a), light points pointed on the arrows represent the bacterial colonies.

Figure 6 - Testing of biological contaminants in the samples: (a) contaminated water for control, (b) Q1, (c) G, (d) V (e) lactic acid (AcL).

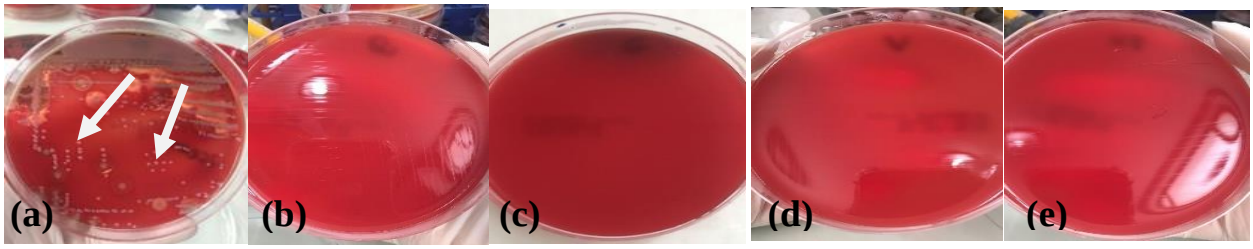

Source: Research Data.

To measure the efficiency of the drug release of the drug vancomycin crosslinking of the base solution in three distinct sequences R1, R2 and R3 the sample was subjected to drug release tests in Table 3. The percentages of the drug released in the hydrogels in the time intervals of 5, 15, 30, 60, 120, 180, 240 and 300 minutes are expressed. It can be observed that after one week (7 days) of hydrogel storage, drug release after 300 minutes was close, indicating that there was no drug degradation due to storage under the conditions performed in this study. Figure 7 shows the kinetic behaviour of drug releases.

Table 3 - Percentage of release of the vancomycin drug.

% Drug releanase						
	R1		**R2**		**R3**	
Time (min)	1ª Reading	2ª Reading	1ª Reading	2ª Reading	1ª Reading	2ª Reading
5	15.62	18.72	20.59	22.64	21.30	30.49
15	35.21	24.13	26.71	48.16	36.51	41.85
30	47.29	48.12	34.58	60.83	41.28	47.07
60	78.47	45.47	60.06	61.43	63.38	70.49
120	75.15	83.63	66.25	74.53	82.44	61.38
180	84.90	76.89	78.12	89.49	75.38	78.60
240	89.17	82.05	96.99	92.94	95.10	93.93
300	87.69	89.38	95.30	87.68	91.21	96.54

Source: Research Data.

Figure 7 - Kinetic profile of the release of the drug vancomycin adsorbed on the hydrogel matrix using the three hydrogel crosslinking sequences. (A) 1st reading (B) 2nd reading.

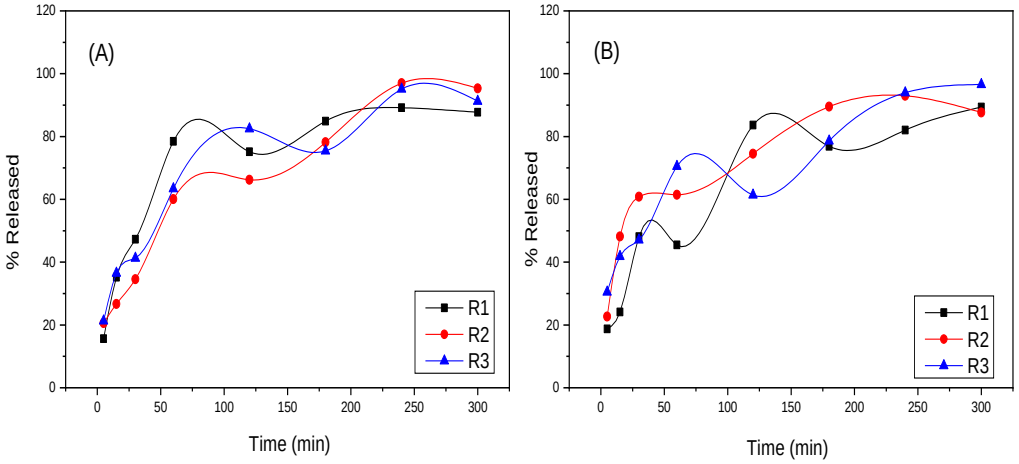

Source: Research Data.

It can be seen in Figure 9, that the drug release behaviour was similar regardless of how it was added, as well as the storage period. It was possible to observe through the kinetic profiles of the drug vancomycin release that initially there was a faster release, within 150 minutes (2.5hrs), and that soon after this period, the release became slower until the end of time observed from 300 min (5hrs). The literature reports that an ideal drug delivery system is one that provides effective doses of drug to the treatment site, acting preventively to protect the biomaterial, preventing adhesion, colonization, biofilm, and subsequently, bacterial proliferation, and that, at the same time, it allows a continuous release over prolonged periods, as the formation of protective fibrous capsules and tissue integration occur in a more distant period of time, weeks to months, after the implantation of the biomaterial (Liu et al., 2002; Neufeld & Bianco-Peled, 2017; P. Wu & Grainger, 2006).

However, the tests performed showed that there was not 100% release of vancomycin even at longer times. The same observation was made by López-Iglesias et al. (2019), when they developed vancomycin-loaded chitosan airgel spheres tested as a potential formulation to treat and prevent wound infections, indicating that this fact may be associated with the drug's interaction with the chitosan structure through hydrogen bonds.

Observation also verified by researcher Zhao et al. (2014), who produced a hydrogel based on chitosan crosslinked with Dextran grafted with maleic acid by the Michael addition reaction, using vancomycin as a drug to prevent wound infections, and observed that as the amount of polysaccharide Dextran decreased in hydrogels, the amount of drug released increased, indicating that there is an interaction between vancomycin/polysaccharide, thus causing changes in the drug release behavior. This may be strongly related to the interaction of the hydroxyl groups present in the vancomycin structure with Dextran.

Figure 8 illustrates photographs of chitosan hydrogels (Q1 and Q2) cross-linked with genipin and the drug vancomycin. It is possible to observe different aspects obtained with the different formulations of hydrogels. Heterogeneous and diffuse appearance, where macroscopically it is not possible to identify the phases present, darker colors that correspond to the first formulations of hydrogels produced with a greater amount of genipin, which provides physical characteristics unsuitable for use in syringes, as they were brittle. During the hydrogel formulations, a lighter color with less crosslinking agent and lower viscosity were obtained.

Figure 8 - Photographs of chitosan hydrogels (Q1 and Q2) cross-linked with genipin and the drug vancomycin.

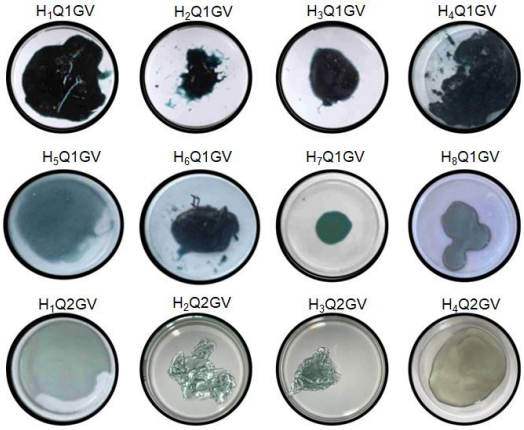

Source: Research Data.

Table 4 presents the hydrogels obtained and their physical characteristics and pH. Through the results obtained, it is that the hydrogel that presented the best result was H5Q1GV, whose pH was 5.7 after 8 h of agitation at 840 RPM and 27°C, as it was homogeneous and with viscosity and ideal adhesion to be used in prostheses, being evaluated with the aid of a syringe.

Table 4 - Physical characteristics and pH of hydrogels.

Hydrogels	pH	Characteristics
HQ1G	3.6	-
HQ2G	4.2	-
H_1Q1GV	3.8	Crumbly
H_2Q1GV	4.5	Crumbly
H_3Q1GV	4.7	Crumbly
H_4Q1GV	-	Homogeneous
H_5Q1GV	**5.7**	**Homogeneous**
H_6Q1GV	-	Crumbly
H_7Q1GV	5.6	Flimsy
H_8Q1GV	5.0	Flimsy
H_1Q2GV	5.4	somewhat inconsistent
H_2Q2GV	5.4	**Homogeneous**
H_3Q2GV	5.7	Crumbly
H_4Q2GV	5.7	Flimsy
H_5Q1GV	5.7	**Homogeneous**

Source: Research Data.

Figure 9 illustrates the infrared spectra of the hydrogels H5Q1G e HRQ1GV with chitosan produced locally CERTBIO Figure 4a and 4b, and H5Q2G E H5Q2GV produced commercially shown in Figure 4c and 4d. respectively, it can be observed that there was an increase in the absorption band of 1649cm-^{1} and an observed deviation related to the same band of 1634cm-^{1} to 1649cm-^{1} corresponding to the elongation vibration of the C=O carbonyl group of the amide groups (amide I), present in the acetylated units of chitosan. The absorption at 1634cm-^{1} related to the elongation of the C=O ring suggests that the carbonyl group present in the genipin structure reacted with the primary amine group of chitosan to form a secondary amide, a characteristic that corroborates the literature (Dimida et al., 2017; López-Iglesias et al., 2019).

Figure 9 - FTIR spectra of hydrogels with chitosan produced CERTBIO (Q1) and sigma-aldrich (Q2): (a) H5Q1G, (b) H5Q1GV, (c) H5Q2G, (d) H5Q2GV.

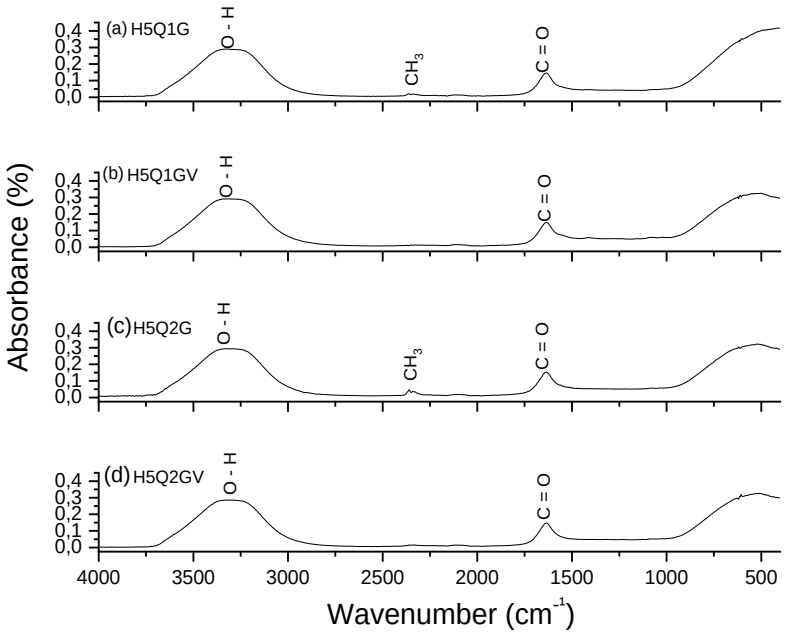

Source: Research Data.

The absorption bands around 1581 and 1589cm^{-1} referring to the deformation vibration of the NH bond of primary amines present in the deacetylated units of chitosan and the aromatic vibration of the CC group present in vancomycin do not appear in the H5Q1GV and H5Q2GV spectra, possibly indicating that there was a reaction between the NH and CC groups of chitosan and vancomycin, respectively. The main bands of vancomycin O-H, C=O, C=C, C-O, C-C were respectively observed at: 3270, 1649, 1490, 1233 and 1589cm^{-1}.

The absorption at 2343cm^{-1} attributed to the CH_3 elongation deformation observed in the genipin spectrum can also be evaluate the H5Q1GV and H5Q2GV Figure 4b and 4d, this absorption at 2343cm^{-1} present in the genipin spectrum was no longer observed which could possibly be associated with a reaction that occurred between the CH_3 group of genipin and some group of vancomycin.

According to Dhawade and Jagtap (2012) and Ordikhani et al. (2014), water forms an intermolecular hydrogen bond with chitosan through the amine and hydroxyl groups, which can cause peak shifts. The hydrogen bond between chitosan and the vancomycin glycopeptide causes only a slight shift in peak position. Therefore, it is suggested that there were no important chemical interactions between the matrix and the drug, which would lead to a structural change in the constituents. The hydroxylic elongation was more pronounced in the hydrogel, which may be associated with the hydrogen bonds present in both chitosan and navancomycin (Yao et al., 2013).

The rheological tests were performed with the H5Q1GV hydrogel showed excellent fluidity when applied to syringes and the results are illustrated in Figure 10. Where, it was found that the H5Q1GV hydrogel presented a pseudoplastic behaviour. This behaviour can be confirmed by the reduction of the apparent viscosity with the increase of the strain rate in Figure 10b and the complex viscosity as a function of the applied oscillation frequency shown in Figure 10c.

Figure 10 - Rheology of the H5Q1GV hydrogel: (a) fluidity in the syringe, (b) flow curve (c) apparent viscosity and (d) complex viscosity.

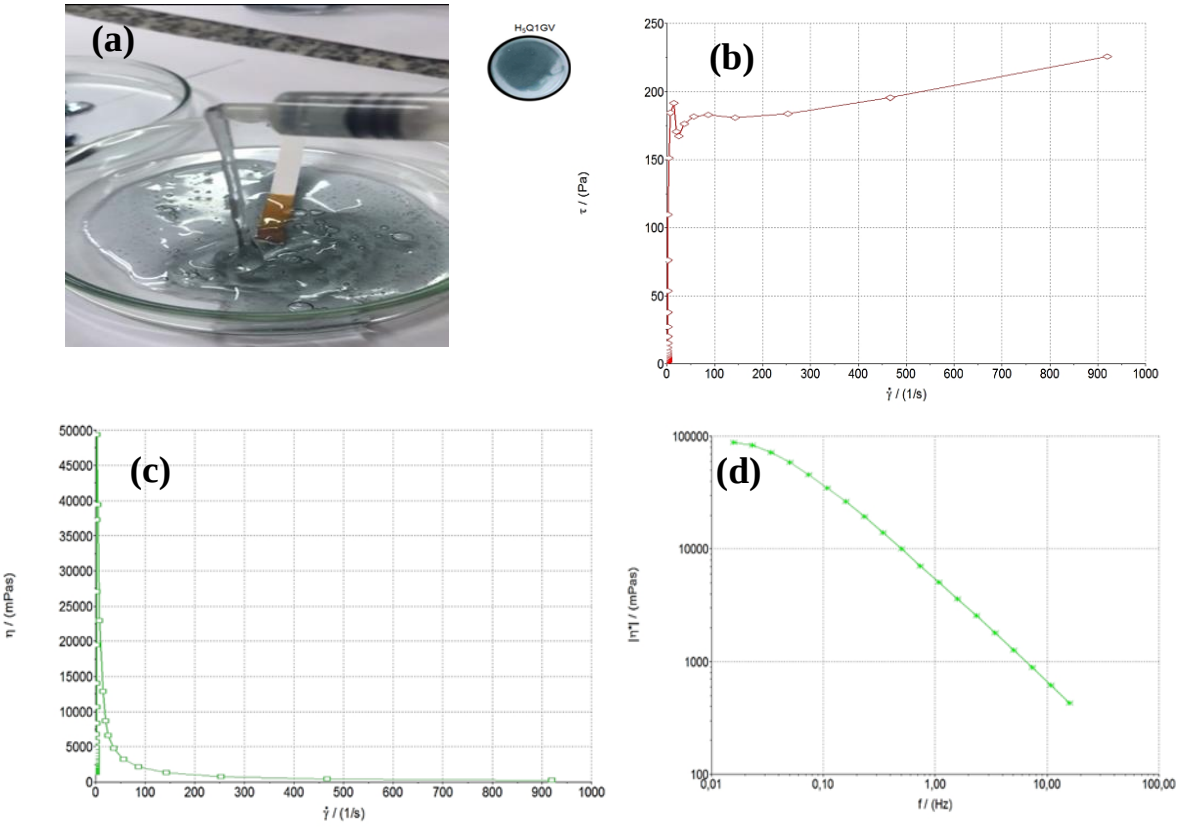

Source: Research Data.

The H5Q1GV hydrogel showed good physical characteristics and homogeneous and with ideal viscosity and adhesion to be used in prostheses, being evaluated with the aid of a syringe. It is important to emphasize that, during the entire production of the hydrogel, due attention was paid to the environment that needed to be closed and refrigerated in order to keep its characteristics preserved and with chances of application in orthopedic surgery.

Regarding the microbiology of the hydrogel, the Kirby-Bauer disk diffusion method was chosen and evaluated the antibacterial activity of the chitosan hydrogel associated with vancomycin used against *Staphylococcus aureus*. The results of the antimicrobial evaluation by (disk diffusion) of the hydrogel, in duplicate, showed at the incubation times of 24 and 48 h that the sample presented antimicrobial activity against the strain used, which can be verified by observing the growth of the inhibition halo or zone of inhibition, which consists of the lighter coloration around the hydrogels, which are associated with chitosan and vancomycin.

Figure 11 illustrates the photographs of the H_5Q1GV hydrogels where the inhibitory halo can be seen at 24 hours and 48 hours of incubation, with the control group without significant halo growth.

Figure 11 – Antimicrobial activity for H5Q1GV: (a) after 24h of incubation and (b) after 48h of incubation. C+V - positive control; HG - hydrogel and C - negative control.

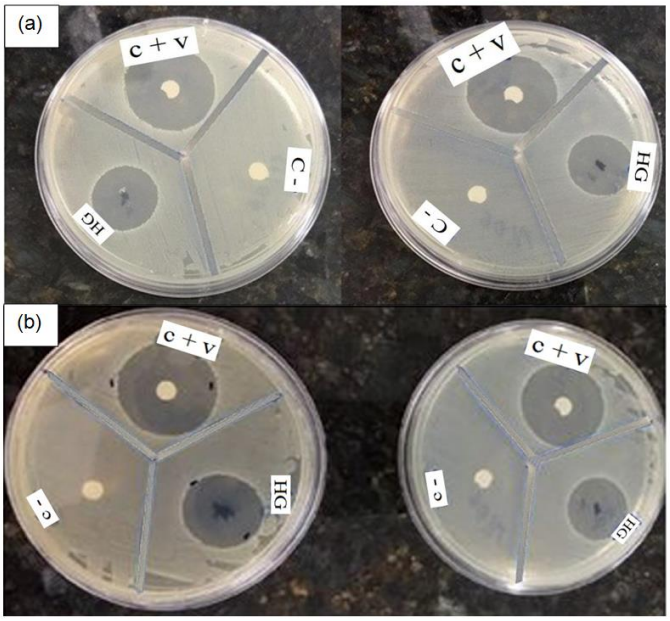

Source: Research Data.

The results of the microbiological tests with the hydrogel show in Figure 11 (a) that the presence of a lighter halo around the HG sample did not allow the growth of bacteria that give an opaquer color as in the negative control sample C- this being the only one that does not have a transparent halo surrounding it. The positive control sample containing the antibiotic vancomycin C+ showed a translucent halo indicating the effectiveness of the released antibiotic to not allow bacterial growth, so although there is a slightly smaller halo, the H5Q1GV hydrogel showed a bactericidal effect like the control carried with vancomycin. The measurement of halos in relation to the incubation time is shown in Table 5. As one of the most reliable methods for analyzing antimicrobial activity, the results obtained were very satisfactory as they show hydrogel halos of approximately 22mm, approaching the standard disc with 29mm vancomycin, means that the hydrogel has an effective antimicrobial effect against the bacteria studied.

Table 5 - Results of antimicrobial assays measuring inhibitory halos.

Sample	Halo diameter 24hrs	Halo diameter 48hrs
Negative Control C-	0	0
Positive Control C + V	29mm	30mm
Hydrogel H5Q1GV	22mm	23mm

Source: Research Data.

As for the cytotoxicity of the hydrogel, after incubation for 24hrs, the wells were macroscopically observed and a clear halo formed around the positive controls, related to the cytotoxicity of the specimen, which did not occur with: H5Q1GV(LI) analyzed sample in triplicate, which did not show the formation of halos, a result similar to the negative control. Therefore, macroscopically the extent of the discolored area (dead cells) of the positive control was measured from the ends in the 4 different quadrants with the aid of a caliper, and the mean value of the values of the 4 different quadrants was calculated. The mean values

obtained for each sample and controls with the specified limits for the different degrees of cytotoxicity indicated in Table 6 and were listed in Table 7.

Table 6 – Degree of cytotoxicity.

DEGREE	CYTOTOXICITY	DESCRIPTION OF THE CYTOTOXICITY ZONE
0	Absent	Absence of discoloration around or under the sample.
1	Light	Bleaching zone limited to the area under the sample.
2	Soft	Size of the bleaching zone from the sample less than 0.45 cm.
3	Moderate	Size of the bleaching zone from the sample between 0.45 cm to 1.0 cm.
4	Severe	Size of the bleaching zone from the sample greater than 1.0 cm, but not involving the entire plate.

Source: Research Data.

Table 7 – Distribution of samples/ Plate reading – samples.

DISTRIBUTION OF SAMPLES ON THE PLATE								
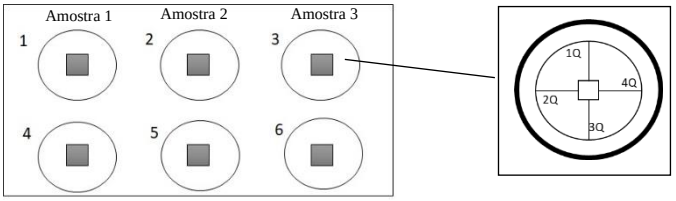								
READING THE PLATES - SAMPLES								
	Orifice/Q*	**1°Q (mm)**	**2Q (mm)**	**3Q (mm)**	**4Q (mm)**	**M**(cm)**	**MG*** (cm):**	**Result**
Sample 1	1	0	0	0	0	0	0.0	☒ Satisfactory ☐ Unsatisfactory ☐ Repeat
	4	0	0	0	0	0		
Sample 2	2	0	0	0	0	0	0.0	☒ Satisfactory ☐ Unsatisfactory ☐ Repeat
	5	0	0	0	0	0		
Sample 3	3	0	0	0	0	0	0.0	☒ Satisfactory ☐ Unsatisfactory ☐ Repeat
	6	0	0	0	0	0		
READING THE PLATES - CONTROLS								
	Orifice/Q*	**1Q (mm)**	**2Q (mm)**	**3Q (mm)**	**4Q (mm)**	**M**(cm)**	**MG*** (cm):**	**Result**
Positive control	1	12	10	09	11	1,05	1.025	☐ Satisfactory ☒ Insatisfatório ☐ Repetir
	4	11	10	10	09	1,0		
	2	0.0	0.0	0.0	0.0	0.0	0.0	

Negative Control	5	0.0	0.0	0.0	0.0	0.0		☒ Satisfactory ☐ Unsatisfactory ☐ Repeat
Blank	3							☐ Satisfactory ☐ Unsatisfactory ☐ Repeat
	6							

Source: Research Data.

The validity of the assay is based on the responses of the cells to the negative control, positive control and blank treatment. The negative control showed no cytotoxic reaction (grade 0), the positive control showed a clear severe cytotoxic reaction (grade 4) and the blank control showed no cytotoxic reaction. From the verification of the absence of halos in the samples, a way to expand the macroscopic visualization of the samples was sought. For this purpose, the wells were photographed microscopically with an inverted digital microscope NIKON TS100 11.05.85 and transferred to a computer to use the NIS-Elements software, with the image magnification resources of this program, it was possible to better identify the limits of the areas in question.

Through an inverted microscope, photos were taken of a region of each well of the analyzed samples, at 100X magnification. From then onwards, the absence of discoloration around and under the samples was found, evidencing the absence of cytotoxicity (Degree 0) as shown in Figure 12, qualifying the sample's cytotoxicity as satisfactory according to ISO 10993–5 (2009).

Figure 12 – Images with 100X magnification of L929 cell lineage of the discoloration zones of experimental materials in the agar diffusion test: positive control (toxic latex) (A), negative control (HDPE) (B), sample H5Q1GV-LI (C).

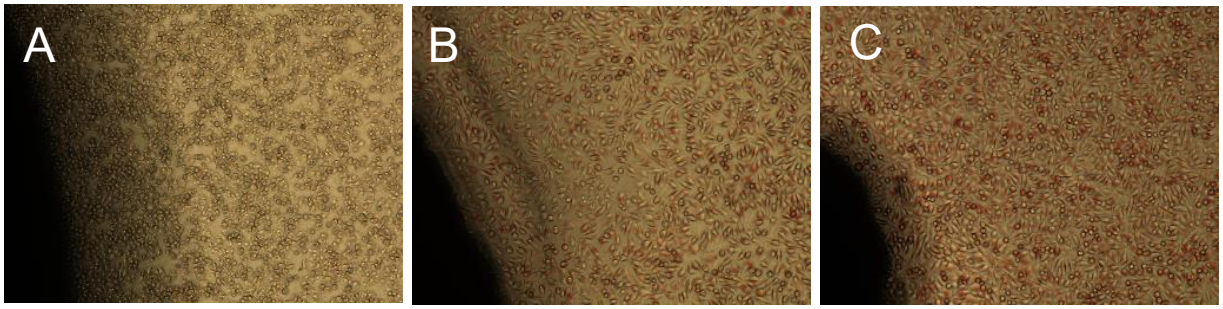

Source: Research Data.

Therefore, the methodology used in this study qualitatively evaluated the cytotoxicity through the extension in cm of the halos and the correlation of the different degrees of cytotoxicity indicated in Table 6 - Degrees of cytotoxicity, also evaluated the cell morphology through the inverted digital microscope NIKON TS100 11.

4. Conclusion

The chitosans used, produced in the laboratory and commercially, showed similar morphological and structural characteristics, producing hydrogels suitable for antimicrobial use in knee prostheses. Genipin as a crosslinking agent proved to be non-toxic, being efficient in the production of hydrogels in the three procedures used.

The drug release in the three crosslinking procedures used proved the effectiveness of drug release in the first hours of product application and after 7 days it presented results close to the initial ones, indicating that there was no drug degradation.

The H5Q1GV hydrogel was successfully obtained, presenting an acid pH of 5.7, which aimed to potentiate the antibacterial effect of chitosan, with the association of the drug vancomycin and in the microbiology assay it was possible to effectively confirm the antimicrobial effect against Staphylococcus aureus presenting a halo capable of preventing the growth of colonies around the hydrogel.

The excellent biocompatibility of the hydrogel indicates its use as a promising adjuvant in the control of nosocomial infections and allows for in vivo assays. Thus, the hydrogel obtained has potential application since the biomaterial produced will prevent bacterial adhesion to the implant, its colonization and subsequent bacterial proliferation. In future works, it is suggested to apply it in the hospital environment and perform pre-clinical evaluation in vivo, aiming to confirm its effectiveness in knee prosthesis surgeries.

Acknowledgments

LabSMac (Laboratory of Synthesis of Ceramic Materials) technical, structural and scientific support. CERTBIO (Laboratory of Evaluation and Development of Biomaterials of the Northeast) technical, structural and scientific support.

References

ANVISA. Agencia Nacional De Vigilância Sanitária. Resolução da diretoria colegiada- RDC nº 17, de 16 de Abril de 2010. www.anvisa.gov.br/legis>

Bakshi, P. S., Selvakumar, D., Kadirvelu, K., & Kumar, N. (2018). Comparative study on antimicrobial activity and biocompatibility of N-selective chitosan derivatives. *Reactive and Functional Polymers*, *124*, 149-155.

Biao, L., Tan, S., Wang, Y., Guo, X., Fu, Y., Xu, F., Zu, Y., & Liu, Z. (2017). Synthesis, characterization and antibacterial study on the chitosan-functionalized Ag nanoparticles. *Materials Science Engineering: C*, *76*, 73-80.

Birt, M. C., Anderson, D. W., Toby, E. B., & Wang, J. (2017). Osteomyelitis: recent advances in pathophysiology and therapeutic strategies. *Journal of orthopaedics*, *14*(1), 45-52.

Cai, Y., Xu, K., Hou, W., Yang, Z., & Xu, P. (2017). Preoperative chlorhexidine reduces the incidence of surgical site infections in total knee and hip arthroplasty: a systematic review and meta-analysis. *International Journal of Surgery*, *39*, 221-228.

Carvalho, C. R., López-Cebral, R., Silva-Correia, J., Silva, J. M., Mano, J. F., Silva, T. H., Freier, T., Reis, R. L., & Oliveira, J. M. (2017). Investigation of cell adhesion in chitosan membranes for peripheral nerve regeneration. *Materials Science Engineering: C 71*, 1122-1134.

Carvalho Júnior, L. H. d., Temponi, E. F., & Badet, R. (2013). Infecção em artroplastia total de joelho: diagnóstico e tratamento. *Revista Brasileira de Ortopedia*, *48*(5), 389-396.

Cats-Baril, W., Gehrke, T., Huff, K., Kendoff, D., Maltenfort, M., & Parvizi, J. (2013). International consensus on periprosthetic joint infection: description of the consensus process. *Clinical Orthopaedics and Related Research®*, *471*(12), 4065-4075.

Chang, T.-Y., Chen, C.-C., Cheng, K.-M., Chin, C.-Y., Chen, Y.-H., Chen, X.-A., Sun, J.-R., Young, J.-J., & Chiueh, T.-S. (2017). Trimethyl chitosan-capped silver nanoparticles with positive surface charge: their catalytic activity and antibacterial spectrum including multidrug-resistant strains of Acinetobacter baumannii. *Colloids Surfaces B: Biointerfaces*, *155*, 61-70.

Cobra, H., Mozella, A. P., Labronici, P. J., Cavalcanti, A. S., & Guimaraes, J. A. M. (2021). Infection after primary total knee arthroplasty: a randomized controlled prospective study of the addition of antibiotics to bone cement. *Revista Brasileira de Ortopedia*
56(5), 621-627.

Cox, S. C., Jamshidi, P., Eisenstein, N. M., Webber, M. A., Hassanin, H., Attallah, M. M., Shepherd, D. E., Addison, O., & Grover, L. M. (2016). Adding functionality with additive manufacturing: Fabrication of titanium-based antibiotic eluting implants. *Materials Science and Engineering: C*, *64*, 407-415.

Delgadillo-Armendariz, N. L., Rangel-Vazquez, N. A., Marquez-Brazon, E. A., & Gascue, R.-D. (2014). Interactions of chitosan/genipin hydrogels during drug delivery: a QSPR approach. *Química Nova*, *37*(9), 1503-1509.

Demetgül, C., & Beyazit, N. (2018). Synthesis, characterization and antioxidant activity of chitosan-chromone derivatives. *Carbohydrate polymers*, *181*, 812-817.

Dhawade, P. P., & Jagtap, R. N. (2012). Characterization of the glass transition temperature of chitosan and its oligomers by temperature modulated differential scanning calorimetry. *Adv Appl Sci Res*, *3*(3), 1372.

Dimida, S., Barca, A., Cancelli, N., De Benedictis, V., Raucci, M. G., & Demitri, C. (2017). Effects of genipin concentration on cross-linked chitosan scaffolds for bone tissue engineering: Structural characterization and evidence of biocompatibility features. *International Journal of Polymer Science*.

Fan, Z., Qin, Y., Liu, S., Xing, R., Yu, H., Chen, X., Li, K., & Li, P. (2018). Synthesis, characterization, and antifungal evaluation of diethoxyphosphoryl polyaminoethyl chitosan derivatives. *Carbohydrate polymers*, *190*, 1-11.

Filipović, U., Dahmane, R. G., Ghannouchi, S., Zore, A., & Bohinc, K. (2020). Bacterial adhesion on orthopedic implants. *Advances in Colloid and Interface*

Science, *283*, 102228.

Florea, D. A., Albuleț, D., Grumezescu, A. M., & Andronescu, E. (2020). Surface modification–A step forward to overcome the current challenges in orthopedic industry and to obtain an improved osseointegration and antimicrobial properties. *Materials Chemistry and Physics*, *243*, 122579.

Geary, M. B., Macknet, D. M., Ransone, M. P., Odum, S. D., & Springer, B. D. (2020). Why Do Revision Total Knee Arthroplasties Fail? A Single-Center Review of 1632 Revision Total Knees Comparing Historic and Modern Cohorts. *J Arthroplasty*, *35*(10), 2938-2943.

Grasso, P., Gaydon, J., & Hendy, R. (1973). The safety testing of medical plastics. II. An assessment of lysosomal changes as an index of toxicity in cell cultures. *Food cosmetics toxicology*, *11*(2), 255-263.

He, M., Han, B., Jiang, Z., Yang, Y., Peng, Y., & Liu, W. (2017). Synthesis of a chitosan-based photo-sensitive hydrogel and its biocompatibility and biodegradability. *Carbohydr Polym*, *166*, 228-235.

Huang, B., Liu, M., & Zhou, C. (2017). Chitosan composite hydrogels reinforced with natural clay nanotubes. *Carbohydrate polymers*, *175*, 689-698.
Hunter, D. J., & Bierma-Zeinstra, S. (2019). Osteoarthritis. *The Lancet*, *393*(10182), 1745-1759.

Ide, W., & Farrag, Y. (2020). Natural Polymeric Materials as a Vehicle for Antibiotics (*Antibiotic Materials in Healthcare* (pp. 51-64). Elsevier.
Iftime, M.-M., Morariu, S., & Marin, L. (2017). Salicyl-imine-chitosan hydrogels: Supramolecular architecturing as a crosslinking method toward multifunctional hydrogels. *Carbohydrate polymers 165*, 39-50.

Jarquín-Yáñez, K., García-Gutiérrez, P., Faustino-Vega, A., Castell-Rodríguez, A. E., Piñón-Zárate, G., Macín-Cabrera, S., Quirino-Barreda, C., & Miranda-Calderón, J. E. (2017). In vitro characterisation of optimised chitosan microparticles loaded with vancomycin by factorial experiment design. *Revista mexicana de ciencias farmacéuticas*, *48*(4), 43-51.

Jeon, S. J., Ma, Z., Kang, M., Galvão, K. N., & Jeong, K. C. (2016). Application of chitosan microparticles for treatment of metritis and in vivo evaluation of broad spectrum antimicrobial activity in cow uteri. *Biomaterials*, *110*, 71-80.

Jóźwiak, T., Filipkowska, U., Szymczyk, P., Rodziewicz, J., & Mielcarek, A. (2017). Effect of ionic and covalent crosslinking agents on properties of chitosan beads and sorption effectiveness of Reactive Black 5 dye. *Reactive Functional Polymers114*, 58-74.

Kapadia, B. H., Elmallah, R. K., & Mont, M. A. (2016). A randomized, clinical trial of preadmission chlorhexidine skin preparation for lower extremity total joint arthroplasty. *The Journal of arthroplasty*, *31*(12), 2856-2861.

Kim, E.-H., Han, G.-D., Kim, J.-W., Noh, S.-H., Lee, J.-G., Ito, Y., & Son, T.-I. (2017). Visible and UV-curable chitosan derivatives for immobilization of biomolecules. *International journal of biological macromolecules*, *104*, 1611-1619.

Kumar, M., Kumar, R., & Kumar, S. (2021). Coatings on orthopedic implants to overcome present problems and challenges: A focused review. *Materials Today: Proceedings*, *45*, 5269-5276.

Lai, J.-Y., Li, Y.-T., & Wang, T.-P. (2010). In vitro response of retinal pigment epithelial cells exposed to chitosan materials prepared with different cross-linkers. *International journal of molecular sciences*, *11*(12), 5256-5272.

Laskar, K., Faisal, S. M., Rauf, A., Ahmed, A., & Owais, M. (2017). Undec-10-enoic acid functionalized chitosan based novel nano-conjugate: An enhanced anti-bacterial/biofilm and anti-cancer potential. *Carbohydrate polymers 166*, 14-23.

Li, B., Shan, C.-L., Zhou, Q., Fang, Y., Wang, Y.-L., Xu, F., Han, L.-R., Ibrahim, M., Guo, L.-B., & Xie, G.-L. (2013). Synthesis, characterization, and antibacterial activity of cross-linked chitosan-glutaraldehyde. *Marine drugs*, *11*(5), 1534-1552.

Lin, X., Yang, S., Lai, K., Yang, H., Webster, T. J., & Yang, L. (2017). Orthopedic implant biomaterials with both osteogenic and anti-infection capacities and associated in vivo evaluation methods. *Nanomedicine*, *13*(1), 123-142.

Liu, S. J., Wen-Neng Ueng, S., Lin, S. S., & Chan, E. C. (2002). In vivo release of vancomycin from biodegradable beads. *Journal of Biomedical Materials Research: An Official Journal of The Society for Biomaterials, The Japanese Society for Biomaterials, and The Australian Society for Biomaterials and the Korean Society for Biomaterials*, *63*(6), 807-813.

Lombardi Jr, A., Berend, K., & Adams, J. (2014). Why knee replacements fail in 2013: patient, surgeon, or implant? *The bone & joint journal*, *96*(11_Supple_A), 101-104.

Long, M. J., Papi, E., Duffell, L. D., & McGregor, A. H. (2017). Predicting knee osteoarthritis risk in injured populations. *Clinical biomechanics*, *47*, 87-95.

López-Iglesias, C., Barros, J., Ardao, I., Monteiro, F. J., Alvarez-Lorenzo, C., Gómez-Amoza, J. L., & García-González, C. A. (2019). Vancomycin-loaded chitosan aerogel particles for chronic wound applications. *Carbohydrate polymers*, *204*, 223-231.

Luo, M., Peng, H., Deng, Z., Yin, Z., Zhao, Q., & Xiong, H. (2015). Preparation and characterization of genipin-crosslinked chitosan microspheres for the sustained release of salidroside. *International Journal of Food Engineering*, *11*(3), 323-333.

Miranda, V. S., Vivielle, B., Machado, L. A., & Dias, J. M. D. (2012). Prevalence of chronic musculoskeletal disorders in elderly Brazilians: a systematic review of the literature. *BMC musculoskeletal disorders*, *13*(1), 1-11.

Mishra, S. K., Ferreira, J., & Kannan, S. (2015). Mechanically stable antimicrobial chitosan–PVA–silver nanocomposite coatings deposited on titanium implants. *Carbohydrate polymers*, *121*, 37-48.

Mohamed, R. R., Elella, M. H. A., & Sabaa, M. W. (2017). Cytotoxicity and metal ions removal using antibacterial biodegradable hydrogels based on N-quaternized chitosan/poly (acrylic acid). *International journal of biological macromolecules 98*, 302-313.

Moura, M. J., Brochado, J., Gil, M. H., & Figueiredo, M. M. (2017). In situ forming chitosan hydrogels: Preliminary evaluation of the in vivo inflammatory

response. *Materials Science Engineering: C 75*, 279-285.

Mozalewska, W., Czechowska-Biskup, R., Olejnik, A. K., Wach, R. A., Ulański, P., & Rosiak, J. M. (2017). Chitosan-containing hydrogel wound dressings prepared by radiation technique. *Radiation Physics Chemistry 134*, 1-7.

Neufeld, L., & Bianco-Peled, H. (2017). Pectin–chitosan physical hydrogels as potential drug delivery vehicles. *International journal of biological macromolecules*, *101*, 852-861.

Ordikhani, F., Tamjid, E., & Simchi, A. (2014). Characterization and antibacterial performance of electrodeposited chitosan–vancomycin composite coatings for prevention of implant-associated infections. *Materials Science Engineering: C*, *41*, 240-248.

Osmani, R. A. M., Singh, E., Jadhav, K., Jadhav, S., & Banerjee, R. (2021). Biopolymers and biocomposites: Nature's tools for wound healing and tissue engineering (*Applications of Advanced Green Materials* (pp. 573-630). Elsevier.

Park, C.-W., Li, X., Vogt, F. G., Hayes Jr, D., Zwischenberger, J. B., Park, E.-S., & Mansour, H. M. (2013). Advanced spray-dried design, physicochemical characterization, and aerosol dispersion performance of vancomycin and clarithromycin multifunctional controlled release particles for targeted respiratory delivery as dry powder inhalation aerosols. *International journal of pharmaceutics*, *455*(1-2), 374-392.

Pawar, V., Bulbake, U., Khan, W., & Srivastava, R. (2019). Chitosan sponges as a sustained release carrier system for the prophylaxis of orthopedic implant-associated infections. *International journal of biological macromolecules*, *134*, 100-112.

Perni, S., & Prokopovich, P. (2020). Nanostructured coatings for antimicrobial applications (*Advances in Nanostructured Materials and Nanopatterning Technologies* (pp. 115-140). Elsevier.

Primorac, D., Molnar, V., Rod, E., Jelec, Z., Cukelj, F., Matisic, V., Vrdoljak, T., Hudetz, D., Hajsok, H., & Boric, I. (2020). Knee Osteoarthritis: A Review of Pathogenesis and State-Of-The-Art Non-Operative Therapeutic Considerations. *Genes (Basel)*, *11*(8).

Qi, C., Rogachev, A., Tapal'skii, D., Yarmolenko, M., Rogachev, A., Jiang, X., Koshanskaya, E., & Vorontsov, A. (2017). Nanocomposite coatings for implants protection from microbial colonization: formation features, structure, and properties. *Surface and Coatings Technology*, *315*, 350-358.

Rahman, Z., & Khan, M. A. (2013). Hunter screening design to understand the product variability of solid dispersion formulation of a peptide antibiotic. *International journal of pharmaceutics*, *456*(2), 572-582.

Raphel, J., Holodniy, M., Goodman, S. B., & Heilshorn, S. C. (2016). Multifunctional coatings to simultaneously promote osseointegration and prevent infection of orthopaedic implants. *Biomaterials*, *84*, 301-314.

Rodríguez-Contreras, A., García, Y., Manero, J. M., & Rupérez, E. (2017). Antibacterial PHAs coating for titanium implants. *European Polymer Journal*, *90*, 66-78.

Sáez, M., Vizcaíno, A., Alarcón, F., & Martínez, T. (2017). Comparison of lacZ reporter gene expression in gilthead sea bream (Sparus aurata) following oral or intramuscular administration of plasmid DNA in chitosan nanoparticles. *Aquaculture474*, 1-10.

Saidykhan, L., Bakar, M. Z. B. A., Rukayadi, Y., Kura, A. U., & Latifah, S. Y. (2016). Development of nanoantibiotic delivery system using cockle shell-derived aragonite nanoparticles for treatment of osteomyelitis. *International journal of nanomedicine*, *11*, 661.

Saikia, C., Das, M. K., Ramteke, A., & Maji, T. K. (2016). Effect of crosslinker on drug delivery properties of curcumin loaded starch coated iron oxide nanoparticles. *International journal of biological macromolecules*, *93*, 1121-1132.

Saita, K., Nagaoka, S., Shirosaki, T., Horikawa, M., Matsuda, S., & Ihara, H. (2012). Preparation and characterization of dispersible chitosan particles with borate crosslinking and their antimicrobial and antifungal activity. *Carbohydrate Research*, *349*, 52-58.

Sami, A. J., Khalid, M., Jamil, T., Aftab, S., Mangat, S. A., Shakoori, A., & Iqbal, S. (2018). Formulation of novel chitosan guargum based hydrogels for sustained drug release of paracetamol. *International journal of biological macromolecules*, *108*, 324-332.

Sedghi, R., Shaabani, A., Mohammadi, Z., Samadi, F. Y., & Isaei, E. (2017). Biocompatible electrospinning chitosan nanofibers: a novel delivery system with superior local cancer therapy. *Carbohydrate polymers 159*, 1-10.

Solé, I., Vílchez, S., Miras, J., Montanyà, N., García-Celma, M. J., & Esquena, J. (2017). DHA and l -carnitine loaded chitosan hydrogels as delivery systems for topical applications. *Colloids and Surfaces A: Physicochemical and Engineering Aspects*, *525*, 85-92.

Standardization, I. O. f. (2009). ISO 10993-5: 2009-Biological evaluation of medical devices-Part 5: Tests for in vitro cytotoxicity. ISO Geneva.
Talebian, A., & Mansourian, A. (2017). Release of Vancomycin from electrospun gelatin/chitosan nanofibers. *Materials Today: Proceedings*, *4*(7), 7065-7069.

Vasilieva, T., Sigarev, A., Kosyakov, D., Ul'yanovskii, N., Anikeenko, E., Chuhchin, D., Ladesov, A., Hein, A. M., & Miasnikov, V. (2017). Formation of low molecular weight oligomers from chitin and chitosan stimulated by plasma-assisted processes. *Carbohydrate polymers*
163, 54-61.

Vivacqua, T., Moraes, R., Barretto, J., Cavanelas, N., Albuquerque, R., & Mozella, A. (2021). Functional Outcome of Patients Undergoing Knee Arthrodesis after Infected Total Arthroplasty. *Revista Brasileira de Ortopedia*, *56*(3), 320-325.

Wahid, F., Wang, H.-S., Zhong, C., & Chu, L.-Q. (2017). Facile fabrication of moldable antibacterial carboxymethyl chitosan supramolecular hydrogels cross-linked by metal ions complexation. *Carbohydrate polymers 165*, 455-461.

Wu, P., & Grainger, D. W. (2006). Drug/device combinations for local drug therapies and infection prophylaxis. *Biomaterials*, *27*(11), 2450-2467.

Wu, S., Dong, H., Li, Q., Wang, G., & Cao, X. (2017). High strength, biocompatible hydrogels with designable shapes and special hollow-formed character using chitosan and gelatin. *Carbohydrate polymers 168*, 147-152.

Xu, Y., Han, J., & Lin, H. (2017). Fabrication and characterization of a self-crosslinking chitosan hydrogel under mild conditions without the use of strong bases. *Carbohydrate polymers 156*, 372-379.

Yang, Y., Yang, S.-B., Wang, Y.-G., Zhang, S.-H., Yu, Z.-F., & Tang, T.-T. (2017). Bacterial inhibition potential of quaternised chitosan-coated VICRYL absorbable suture: An in vitro and in vivo study. *Journal of orthopaedic translation 8*, 49-61.

Yao, Q., Nooeaid, P., Roether, J. A., Dong, Y., Zhang, Q., & Boccaccini, A. R. (2013). Bioglass®-based scaffolds incorporating polycaprolactone and chitosan coatings for controlled vancomycin delivery. *Ceramics International*, *39*(7), 7517-7522.

Yousaf, S. S., Houacine, C., Khan, I., Ahmed, W., & Jackson, M. J. (2020). Importance of biomaterials in biomedical engineering (*Advances in Medical and Surgical Engineering* (pp. 151-177). Elsevier.

Zeng, D.-M., Pan, J.-J., Wang, Q., Liu, X.-F., Wang, H., & Zhang, K.-Q. (2015). Controlling silk fibroin microspheres via molecular weight distribution. *Materials Science and Engineering: C*, *50*, 226-233.

Zhang, Y., Meng, F.-C., Cui, Y.-L., & Song, Y.-F. (2011). Enhancing effect of hydroxypropyl-β-cyclodextrin on the intestinal absorption process of genipin. *Journal of agricultural and food chemistry*, *59*(20), 10919-10926.

Zhao, Y., Zhang, X., Wang, Y., Wu, Z., An, J., Lu, Z., Mei, L., & Li, C. (2014). In situ cross-linked polysaccharide hydrogel as extracellular matrix mimics for antibiotics delivery. *Carbohydrate polymers*, *105*, 63-69.

Zubareva, A., Shagdarova, B., Varlamov, V., Kashirina, E., & Svirshchevskaya, E. (2017). Penetration and toxicity of chitosan and its derivatives. *European Polymer Journal*, *93*, 743-749.